

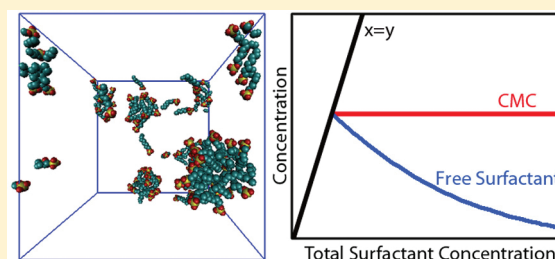
Atomistic Simulations of Micellization of Sodium Hexyl, Heptyl, Octyl, and Nonyl Sulfates

Samantha A. Sanders,[†] Maria Sammalkorpi,^{‡,§} and Athanassios Z. Panagiotopoulos^{*,†}

[†]Department of Chemical and Biological Engineering and Institute for the Science and Technology of Materials, Princeton University, Princeton, New Jersey 08544, United States

[‡]Department of Chemistry, Aalto University, FI-00076 Aalto, Finland

ABSTRACT: Molecular dynamics simulations have been used to study the micellization behavior of atomistic models for sodium alkyl sulfates in explicit water. A major finding of the present work is the observation of a strong dependence of free surfactant concentration on overall surfactant concentration, that has not been reported previously and that is key to comparing simulation results for the critical micelle concentration (CMC) to experimental data. The CMC and aggregate size distributions were obtained for alkyl tail lengths from six to nine at temperatures from 268 to 363 K, from 400 ns simulations covering a number of surfactant and water model combinations. The free surfactant concentration is much lower than the critical micelle concentration for strongly micellizing systems at the relatively high concentrations accessible by simulations. Thus, counterion association must be accounted for in determining the CMC from the raw simulation data. Simulation results are in qualitative agreement with experimental trends for aggregate size and CMC as functions of alkyl tail length and temperature.



1. INTRODUCTION

Surfactants are molecules that consist of hydrophilic “head” groups covalently bonded to hydrophobic “tail” groups. These molecules can assemble into a variety of microstructures, depending on their architecture and external thermodynamic conditions. Their ability to self-assemble leads to their widespread use of surfactants in a variety of applications, including drug delivery^{1,2} and carbon nanotube separation.^{3,4} Understanding how to control the self-assembly process is of great interest for both fundamental and technological reasons. Computer simulations can aid in clarifying how the self-assembly process operates at a microscopic level, depending on macroscopically controlled parameters such as temperature and concentration.

Some of the earliest simulations of amphiphilic systems were done with simple lattice models.⁵ Lattice models with the Monte Carlo method have been used for studying equilibrium properties such as the critical micelle concentration (CMC).^{6–13} Using nonlattice systems and molecular dynamics to study self-assembly and micellization properties has become more prevalent as computational power has increased over the years.^{14–45} Many simulations start from preassembled micellar structures.^{18–27} Although such a setup provides insight into surfactant dynamics and structural properties, the inherent assumption in using a preassembled structure is that the initial configuration resembles a structure close to the global energy minimum. A random initial configuration relaxes this assumption and allows a system to reach—in principle—a variety of possible microstructures. However, when starting from dispersed initial configurations, it can be difficult to

simulate for a sufficient time to achieve equilibration. For example, in previous work by Sammalkorpi and co-workers for sodium dodecyl sulfate,^{29–31} formation of micelles was observed, but the aggregates were still evolving at the end of the 200 ns simulation time; equilibrium properties could not be obtained.

Advanced simulation techniques such as replica exchange⁴⁵ have been employed to attempt to speed up equilibration of self-assembling systems. Models have been adapted for this purpose as well. For example, coarse-grained models^{33–42} and implicit-solvent models^{43,44,46,47} have been used to decrease the computational cost for reaching longer timespans. However, coarse-grained models have difficulty matching aggregation time scales and suffer from loss of transferability across temperatures.⁴⁸ Many coarse-grained models also lack the ability to describe solvent orientation, which can make it impossible to match properties that depend on hydrogen bonding, such as the minimum in the CMC with respect to temperature.^{45,49} Implicit-solvent models can also have difficulty capturing accurate dynamics.⁴³ Ultimately, the goal is to use models accurate enough to reproduce quantitatively all self-aggregation thermodynamic and kinetic properties. Atomistic models with explicit solvent and ions are the most likely candidates for this purpose. For example, Marrink and co-workers have simulated the self-assembly of a single dodecylphosphocholine micelle using an atomistic model and

Received: September 23, 2011

Revised: December 22, 2011

Published: January 31, 2012

were able to compare kinetic constants directly to experiment.²⁸ However, it is not fully known how well atomistic models reproduce equilibrium experimental properties of surfactant self-assembly; this is a key goal of the present study, which probes the dependence of micellar aggregate properties, at or near equilibrium, on overall surfactant concentration and temperature for an atomistic model of sodium alkyl sulfates. Also of interest to the present work is the influence of force field parameters on micellization properties.

The remainder of this paper is organized as follows. We first provide a detailed description of the computational models in section 2.1, simulation conditions in section 2.2, and analysis methods in section 2.3. Results for the dependence of the CMC and aggregate size on temperature, concentration, and alkyl tail length are presented in section 3 along with a comparison between the different models. In the final section, we summarize our findings and comment on possible future extensions of this work.

2. MODELS AND METHODS

2.1. Models. The main model used in the simulations was developed by Sammalkorpi and co-workers,²⁹ with most of its parameters obtained from the earlier GROMOS87 force field.⁵⁰ The model uses a united atom parametrization and SPC water⁵¹ and reproduces experimental results of sodium dodecyl sulfate micelle structure, ionization degree, and hydration.²⁹ We refer to this surfactant/water model combination as our “base model”, while “base surfactant model” refers only to the surfactant part.

In order to test the effect of the model parameters on micellization properties, we simulated several other surfactant/water model combinations. The two additional tested sodium octyl sulfate models use the same functional form as the base surfactant model for the dispersion interactions (Lennard-Jones 12–6 potential) and the same partial charges for the headgroup.⁵² In the first variation of the base surfactant model, TraPPE parameters for CH₂ and CH₃ groups⁵³ are used for the alkyl tail. Lorentz–Berthelot combining rules are used for interactions involving the alkyl tail beads and geometric rules for all other interactions. The bond length of O–CH₂ was fixed at 0.141 nm.⁵⁴ The angle potential parameters for O–CH₂–CH₂ were $\theta_0 = 111^\circ$ and $k_\theta = 293.5$ kJ/(mol rad²) for the harmonic angle potential, $U_{\text{angle}} = (1/2)k_\theta(\theta - \theta_0)^2$. These parameters are originally from the O–C–CH₃ bending angle in ref 55. The Ryckaert–Bellemans parameters for the O–CH₂–CH₂–CH₂ are $C_0 = 6.9831$ kJ/mol, $C_1 = 17.7362$ kJ/mol, $C_2 = 0.8870$ kJ/mol, and $C_3 = -25.6062$ kJ/mol and were calculated from the CH_x–CH₂–CH₂–O parameters in ref 54. All other bond lengths, angle potentials, and dihedral potentials are the same as the base model. We refer to this surfactant model as G-TraPPE. For the second tested sodium octyl sulfate model, we use parameters from Cheng and co-workers that were originally developed for sodium dodecyl sulfate.⁵⁶ The different alkyl chain length parameters are obtained by decreasing/increasing the number of methyl groups in the tail without modifying any other parameters. Major differences between the base surfactant model and these two additional tested models are summarized in Table 1.

The base surfactant model was also simulated in TIP4P/2005 water,⁵⁷ and G-TraPPE was simulated in both SPC⁵¹ and TIP4P/2005 water, in order to determine possible effects of the solvent model. The TIP4P/2005 model was selected for study because it provides a good description of vapor–liquid

Table 1. Model Parameters and Global Cutoff for Intermolecular and Electrostatic Interactions

		model		
		base	G-TraPPE	Cheng
CH ₃	σ (nm)	0.3786	0.375	0.375
	ϵ (kJ/mol)	0.7533	0.8148	0.8148
CH ₂	σ (nm)	0.3965	0.395	0.395
	ϵ (kJ/mol)	0.5856	0.3825	0.3825
OM ^a	σ (nm)	0.2626	0.2626	0.315
	ϵ (kJ/mol)	1.724	1.724	0.8368
Na	σ (nm)	0.2575	0.2575	0.2160
	ϵ (kJ/mol)	0.061 77	0.061 77	1.475
global cutoff (nm)		1.0	1.4	1.5

^aOM beads are the three oxygens connected to only sulfur.

equilibria, liquid properties, and critical properties of water.^{58–61} The Cheng model was parametrized with the SPC/E water model.⁶² For consistency, we simulated it with the SPC/E water model. The Na ion in this model was optimized specifically for SPC/E.⁶³

All model combinations except for the base model were simulated with standard long-range corrections to the energy and pressure for the dispersion (Lennard-Jones) interactions at distances beyond the cutoffs listed in Table 1.

2.2. Systems Studied. The sodium hexyl sulfate surfactant (S6S) that was studied in our previous work⁶⁴ is weakly micellizing, as evidenced by its high CMC, small aggregation number, and lack of separation between oligomer and micelle peaks in the aggregate size distribution. This can make determination of micellization properties ambiguous in both experiments and simulations. In the present study, we focus primarily on sodium octyl sulfate (S8S), which has stronger micellization but still has a relatively high CMC (110–130 mM at 298 K^{65,66}). A high CMC indicates a significant amount of free surfactant in the system and frequent exchanges between micelles and solution, leading to rapid equilibration.^{68,69} In order to investigate the effects of alkyl chain length on the aggregation properties, both lower alkyl chain lengths (hexyl, S6S, and heptyl, S7S) and higher (nonyl, S9S) were also simulated for selected conditions.

For the molecular dynamics simulations, we used the open source package GROMACS 4.⁷⁰ The simulations were performed at a constant pressure of 1 bar using the Parrinello–Rahman barostat^{71,72} with $\tau_p = 5.0$ ps and at constant temperature using the Nose–Hoover thermostat⁷³ with $\tau_T = 0.5$ ps. Periodic boundary conditions were used, and the electrostatic interactions were calculated using particle mesh Ewald summation.^{74,75} All simulations used a time step of 2 fs and a frame output rate of 50 ps. Unless otherwise noted, each simulation was 400 ns in length and analysis was performed on the last 300 ns of the run. Specifically for sodium nonyl sulfate (S9S), which has slower equilibration, analysis was performed on the last 200 ns.

To obtain temperature-dependent properties for the base S8S model, simulations were performed at temperatures of 268, 278, 298, 313, 323, 343, and 363 K and at a concentration close to 1 M. The “1 M” S8S systems contained 200 surfactant molecules and 8434 water molecules; density variations with temperature lead to small deviations of the actual concentration from the nominal 1 M value. The simulations for the other model combinations were also done at 298 K with the same system size as for the 1 M S8S base model system. Additional

S8S simulations were performed at 298 K with nominal concentrations of 500 and 250 mM. The 500 mM system contained 200 surfactant molecules and 20 034 water molecules. The 250 mM system contained 100 surfactant molecules and 20 468 water molecules. In order to study the alkyl tail length dependence, simulations were performed at 298 K and a concentration of 1 M for sodium hexyl sulfate (S6S), sodium heptyl sulfate (S7S), and sodium nonyl sulfate (S9S), using the base model. All systems had 200 surfactant molecules. The number of water molecules was 8770, 8602, and 8266 for S6S, S7S, and S9S, respectively. The number of water molecules varies to compensate for slight density differences for surfactants of different length, so as to keep the concentration (in mol/L) constant. Initial conditions for the systems were random distributions of the surfactant molecules, energy minimized using the steepest descent algorithm in GROMACS.

2.3. Analysis Methods. The aggregate size distributions were determined from the trajectory frames. Two surfactant molecules were considered to be part of the same aggregate if any of their carbon tail beads were within 0.41 nm of each other. This cutoff was determined from visual inspection of sodium octyl sulfate simulations and validated from the agreement between CMC values obtained at different concentrations. Production parts of the simulation were divided into five 60 ns blocks (40 ns blocks for S9S). For each segment, an error function, $\phi = \sum_{i=1}^6 (n_i^{\text{gamma}} - n_i^{\text{agg}})^2$, was minimized between the first six points of the aggregate size distribution and a gamma distribution where n is the value of the i th point for the respective distribution. The surfactant concentration represented by the gamma function approximates the free surfactant (nonaggregated) concentration.⁶⁴ Using more than six points in the gamma distribution fitting does not make a significant difference to the calculated CMC values. In the past, we have used the free surfactant concentration as an approximation of the CMC. However, we found here that the free surfactant concentration in the strongly micellizing ionic surfactant systems decreases rapidly with overall surfactant loading and is not representative of the concentration of surfactant present when the first micelle forms. This decrease has also been observed experimentally^{76–78} and in other simulation studies.^{7,10,79} The decrease is attributed to an excluded volume effect as well as to the fact that the free counterions create an effect similar to adding excess salt to the system. For this reason, in the present work we use the following semiempirical expression to relate the total surfactant concentration, C_T , and the free monomer concentration, m_f , to the CMC:

$$\log(m_f) = (1 + \alpha) \log(\text{CMC}) - \alpha \log\left(\frac{(1 - \alpha)(C_T - m_f) + m_f}{1 - VC_T}\right) \quad (1)$$

In eq 1, V is the molar volume of the anhydrous surfactant in L/mol (which was assumed to correspond to a density of 1.0 g/mL) and α is the fraction of counterions associated with the micelles, rather than being free in solution. This expression was initially developed by Quina and co-workers⁸⁰ and later modified to account for the excluded volume effect.^{81,82} We consider oligomers to be included in the free surfactant concentration. The degree of counterion attachment, α , was determined from trajectory configurations using a simple cutoff distance obtained from the first minimum after the highest peak

of the radial distribution function between sodium and sulfur ions. While the exact position of the minimum varies slightly from system to system, a common value of 0.68 nm was chosen for simplicity. Configurations were analyzed to determine the fraction of ions within the cutoff distance of sulfur atoms which were participating in micellar aggregates. Since we were matching the first six points of the aggregate size distribution for the free surfactant concentration, micellar aggregates were defined as clusters of size 7 or greater. The fraction of ions within the cutoff distance is the degree of counterion attachment, α , in eq 1. In addition to the semiempirical eq 1 used here, another theoretical approach⁹³ has recently been developed for calculating the CMC from simulation data at higher concentrations. This approach is based on a hydrophobic theory applied to nonionic surfactants and combined with a Debye–Huckel approximation to account for the electrostatic contributions in the micellization.

The α values obtained are insensitive to temperature but do vary with alkyl tail length and concentration. At 298 K, for the 1 M base model systems, the α values (which have statistical uncertainties of ± 0.01) were 0.63, 0.67, 0.70, and 0.72 for S6S, S7S, S8S, and S9S, respectively. The trend of increasing counterion association with increasing alkyl tail agrees with experiment.⁸³ The α values were 0.55 for the 500 mM and 0.43 for the 250 mM S8S base model systems, respectively. The 250 mM value was still increasing at the end of the simulation, and thus we used the average value of the last 60 ns of the run instead of the block values over the last 300 ns as for the others. The degree of counterion attachment is frequently considered to be constant with respect to concentration,^{80,82} but our results agree with the trend of the experimental trends of Hsiao et al.,⁸⁴ which indicate that as the total surfactant concentration decreases to the cmc, α decreases from a constant value to zero. For sodium dodecyl sulfate,⁸⁴ this decrease occurs when the total surfactant concentration is less than 5 times the CMC (~ 40 mM). The CMC values obtained from eq 1 are not too sensitive to the value of α within the range of 0.4–0.8. The sensitivity generally falls within the statistical uncertainty of the simulations, with the 1 M system being potentially the most sensitive, but also having the best equilibrated α value. For the remainder of this work, we obtain CMC values “locally” from eq 1, using the α values and free surfactant concentrations measured at a given total surfactant loading. Reported statistical uncertainties are the standard deviation of the block averages divided by $\sqrt{n - 1}$ for the standard error of the mean and multiplying the standard error by 3 for a confidence interval of 99.7%.

The need to take into account counterion association becomes clear when analyzing the concentration dependence of the free surfactant concentration and the calculated CMCs. Figure 1 shows that the free surfactant concentration varies significantly with the total surfactant concentration. At the highest total surfactant concentration of ~ 1 M, the free surfactant concentration is 100 times smaller than the CMC in the S8S system at 298 K. Using eq 1 with the measured values of α at each total concentration, CMC values are obtained that show no significant variation with overall surfactant concentration. This is one of the key results of the present study, that has also been confirmed in a recent study of coarse-grained models of sodium alkyl sulfates⁸⁵ and that used a more sophisticated treatment of the counterion association effects.⁹³

2.4. Equilibration. To test equilibration of the simulations, we performed simulations starting from energy-minimized

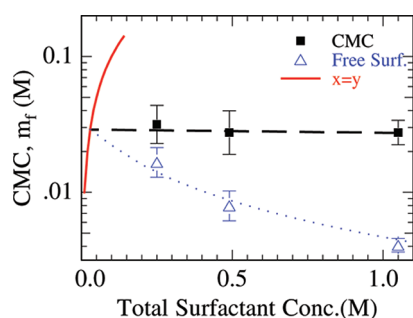


Figure 1. Free surfactant concentration and calculated CMCs as functions of total surfactant concentration for S8S in the base model at 298 K. The solid line is from the relationship $x = y$, and the dotted blue line is from eq 1, assuming a logarithmic dependence of α on total concentration and a CMC of 29 mM. Triangles are the measured free surfactant concentrations and squares the CMCs obtained locally from eq 1. The dashed black line is a linear interpolation from the 1 M CMC data point to the 29 mM point on the $x = y$ line.

random distributions of the surfactant molecules and—for selected systems—from already aggregated configurations. This test was performed on the 1 M sodium octyl sulfate at 298 K and for systems most likely to have slow equilibration because of low temperature (268 K), low concentration (250 mM), or longer alkyl tail length ($n = 9$). The calculated CMCs were found to be independent of starting configuration for each of these systems, indicating that the free surfactant concentration reaches equilibrium for all the systems simulated.

A more stringent test for equilibration is the time evolution of the aggregate size distributions. Typically, the aggregate size distribution stabilizes (aggregates stop growing) within 100 ns, but for the S9S system, the S8S system at $T = 268$ K, and the 250 mM S8S system even 400 ns was found to be insufficient for equilibration. However, the free surfactant concentration was stabilized, and the peak position of the aggregate distribution was changing only slowly; we use data from 300 ns onward for these systems as an approximation of the equilibrium aggregate size distribution for the analysis. For 500 mM S8S, data from 200 ns onward are used for the aggregate size analysis. Typical size distributions for the base S8S system at 298 K are shown in Figure 2 at three different overall

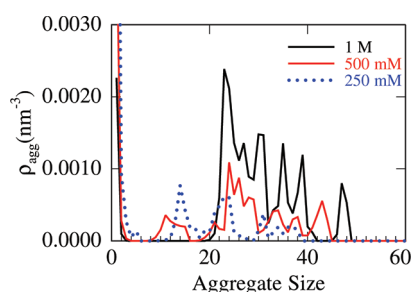


Figure 2. Concentration dependence of the aggregate size distributions for S8S in the base model at 298 K. Black thick solid line: 1 M; red thin solid line: 500 mM from 200 to 400 ns; blue dotted line: 250 mM from 300 to 400 ns. The aggregate distribution for the 250 mM system is still slowly evolving toward larger aggregates.

concentrations. The aggregate size distributions are still somewhat noisy, indicating insufficient sampling, but the overall trend with concentration is clear. In particular, the size of micellar aggregates becomes larger as the total

concentration increases, in agreement with experimental data⁸⁶ and coarse-grained model simulations.⁸⁵ Peaks in the distribution represent relatively stable micelles. Even though surfactant molecules are entering and leaving individual micelles over the course of the simulation, the time required to achieve full equilibration of the aggregate size distributions for these systems significantly exceeds the 400 ns of the present study.

2.5. Cutoff Sensitivity. We tested cutoffs for determining micellar aggregates between 0.40 and 0.45 nm for the S8S base model. With a 0.40 nm cutoff, there are times where nominally “free” surfactants do not appear to be completely separate from the aggregates. At the other extreme, a 0.45 nm cutoff leads to visual agreement of the free surfactant population but increases the probability of two fairly distinct aggregates being considered as a single one. In addition, this higher cutoff leads to a strong variation of the calculated CMCs for different total surfactant concentrations. Changing from a 0.40 nm cutoff to a 0.41 nm cutoff to a 0.45 nm cutoff causes the apparent CMC value to decrease from 49 ± 4 to 27 ± 3 to 18 ± 4 mM at 1 M. However, at $C_T = 250$ mM, there is no significant change: the CMC values obtained are 37 ± 7 , 33 ± 7 , and 32 ± 8 mM, respectively. The cutoff of 0.41 nm is the smallest value that provides visual agreement and agreement of the CMC values between simulations of different total surfactant concentration and was the value used for the remainder of this work.

3. RESULTS AND DISCUSSION

3.1. Temperature Dependence. Figure 3 presents the calculated CMCs at different temperatures. For the smaller

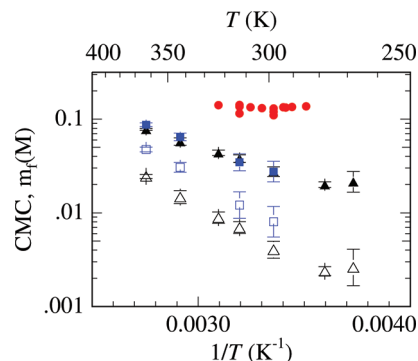


Figure 3. Temperature dependence of the CMC and free surfactant concentration for the S8S base model. Black filled triangles: 1 M CMC; black open triangles: 1 M free surfactant; blue filled squares: 500 mM CMC; blue open squares: 500 mM free surfactant; filled red circles: experimental CMC data from refs 65, 66, and 86–89.

surfactant concentration of 500 mM it is harder to reach equilibrium at lower temperatures, so only high-temperature data were obtained; the corrected CMC values from both concentrations are in good agreement over the temperature range at which both are available. At higher temperatures ($T > 300$ K), the increase of the CMC with temperature is steeper than the weak dependence seen experimentally. At lower temperatures, experiments suggest a weak minimum in the CMC around 298 K.⁶⁶ This is a feature that is difficult for coarse-grained models to capture because it is related to how water organizes itself in a temperature-dependent network of hydrogen bonds.⁴⁹ In the present study, which uses an atomistic model with explicit water, we observe a minimum

in the CMC around 278 K, even though the large statistical uncertainty of the data at the lowest temperature prevents us from making a definite determination. It is clear from the data, however, that the strong dependence of the CMC on temperature seen at higher temperatures is no longer present near room temperature, in agreement with experiments. In the future, it may be possible to adjust the temperature of the minimum by changing the interactions between headgroups and solvent. We observe that the base model underpredicts the CMC even after adjusting for the counterion association, by a factor of ~ 4 for S8S, as seen in Figure 3.

The 1 M aggregate size distributions are shown in Figure 4 as functions of temperature (the curve for 298 K has already been

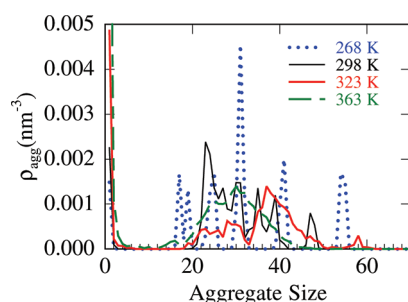


Figure 4. Temperature dependence of aggregate size distributions for the 1 M S8S base model. Blue dotted line: 268 K from 300 to 400 ns; black thick solid line: 298 K; red thin solid line: 323 K; green dashed line: 363 K.

shown in Figure 2). Relatively smooth distributions are achieved at higher temperatures. This is expected because at higher temperatures, more free surfactant is available for exchange between aggregates and bulk solution, so that dynamics of exchange are faster. There is not much variation in the range of aggregate size with the bulk of the aggregates between 20 and 50. These values are in agreement with the experimental value of 27 at 298 K.⁶⁸ The smaller aggregates found at 268 K are likely due to the difficulty in equilibrating the aggregate sizes at low temperatures.

3.2. Alkyl Tail Length Dependence. Figure 5 presents the logarithm of the calculated CMC values as a function of the

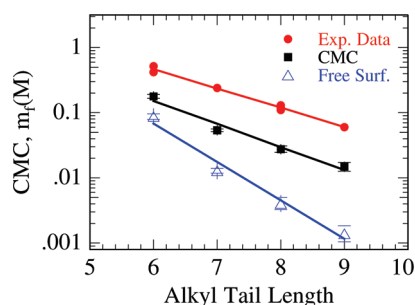


Figure 5. CMC and free surfactant concentration dependence on alkyl tail length for the base model at 298 K and 1 M. Black filled squares: CMC; blue open triangles: free surfactant; red filled circles: experimental data from refs 65–67. Lines are linear least-squares fits to the corresponding points.

alkyl chain length for the studied models. The logarithm of the calculated CMC values decreases with approximately the same slope as the experimental values. However, the free surfactant concentration at 1 M decreases much more rapidly with

increasing alkyl tail length relative to the experimentally measured CMCs. Thus, if the free surfactant concentration were to be used as a direct proxy for the CMC, this would result in increasing discrepancies as the alkyl tail length increases. Unfortunately, this has been common practice in previous simulation studies, including our own prior work.⁶⁴ Because sodium hexyl sulfate has the highest CMC of all systems studied, the correction due to eq 1 is relatively small. We do note that the base model is able to capture the trend of the CMC with respect to the alkyl tail length.

The aggregate size distributions for surfactants of different tail length are shown in Figure 6 (the curve for S8S has already

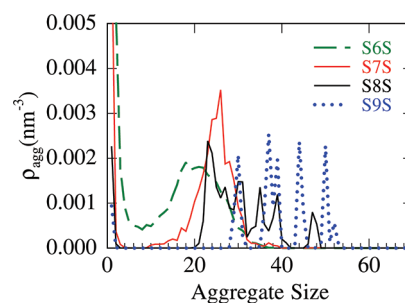


Figure 6. Alkyl tail length dependence of the aggregate size distributions for the base model at 298 K and 1 M total concentration. Green dashed line: S6S; red thin solid line: S7S; black thick solid line: S8S; blue dotted line: S9S from 300 to 400 ns.

been shown in Figure 2). Relatively smooth distributions, indicating full equilibration, are obtained only for S6S and S7S, which have higher CMCs. The trend is clearly an increase in the aggregate size with alkyl chain length, in agreement with experiment^{68,86} and simple geometric theories of surfactant aggregation.⁹⁰

3.3. Model Dependence. We compared the CMC for S8S at 298 K obtained from different model combinations to investigate the sensitivity of the predictions with respect to the intermolecular potential model parameters. Statistically significant differences in the CMC between the GROMOS87 parameters and the TraPPE parameters can be seen in Table 2.

Table 2. Comparison of CMC Values Using Different Model Combinations for 1 M S8S at 298 K

model	cmc (mM)
base	27 ± 3
G-TraPPE/SPC	44 ± 11
base surfactant/(TIP4P/2005)	35 ± 13
G-TraPPE/(TIP4P/2005)	51 ± 10
Cheng/(SPC/E)	43 ± 8

No statistically significant difference between the SPC and TIP4P/2005 water models when combined with the base surfactant model is observed in our simulations. However, the G-TraPPE surfactant in TIP4P/2005 water has a CMC greater than that of the base model. We also tested the recent Cheng model, which contains modifications to the headgroup and ion parameters, using the SPC/E water model. This combination also shows a significant increase in the CMC relative to the base model. This increase is likely due to the use of the TraPPE potential for the alkyl tail, rather than the other adjustments made. The Cheng model has larger aggregates (not shown) compared to the other models, with a range of sizes between 20

and 60. This could be due to the decrease in ϵ of the oxygen atoms for the Cheng model which decreases the repulsion between the head groups and allow for larger aggregates. The other combinations of models give aggregates in the same range as for the base S8S model already shown in Figure 2.

4. CONCLUSIONS

We have studied sodium alkyl sulfate micellization and equilibrium micelle structures using molecular dynamics simulations. To our knowledge, these are the first atomistic simulations of strongly micellizing ionic surfactant systems with explicit solvent and counterions that achieve time scales required for equilibration over a range of temperatures—previous simulation studies were for fast-equilibrating, weakly micellizing systems (e.g., ref 64), or did not reach equilibrium. The effects of alkyl tail length on the CMC and aggregate size were found to be consistent with experimental data. As computational power and software advance, we expect atomistic simulations to provide insight on how models can be improved and to improve our capability to simulate quantitatively complex aggregation phenomena.

A key finding of the present study is that the free surfactant concentration, previously used as a proxy for the CMC, decreases strongly at higher overall surfactant concentrations, in agreement to experimental observations.^{76–78} The free surfactant concentration can be used as an approximation of the CMC only at concentrations near the CMC itself. Practical considerations related to system size and computational resources, however, preclude simulations of very dilute systems. Thus, for strongly micellizing systems such as the ones studied here, an extrapolation of the measured free surfactant concentration to the CMC is necessary to allow comparisons to experimental data. The physical origin of this strong dependence is primarily the “salting out” effect of free counterions. Thus, association between micelles and counterions also needs to be taken into account in correcting for this effect.

All models studied underpredict the experimental CMCs by factors between 2 and 4. While promising, these results suggest that further model refinements are necessary for quantitative agreement of predicted micellization properties with experiments. However, the models reproduce the dependence of CMC on the alkyl tail length. Similar CMC values were obtained with all the tested models, but TRaPPE parameters for the alkyl tail and relatively strong headgroup parameters show the most promise. We note that TRaPPE developers generally favor the TIP4P water model^{94–96} whereas TIP4P/2005, a potential optimized on condensed phase water properties over a wide range of conditions, was used in this work. The TRaPPE surfactant model prediction for the CMC could be somewhat better when used with the original TIP4P water model. In this work, we did not address the influence of the counterion parametrization on the model behavior, which can be significant.⁹¹ An accurate treatment of ions may require nonadditivity of sizes as well as polarizability.⁹²

Simulations similar in spirit to the ones of the present study have recently been completed using a coarse-grained model for sodium alkyl sulfates.⁸⁵ Multiple microsecond time scale simulations for S6S, S9S, and S12S at total surfactant concentrations of 130, 363, and 1005 mM were performed, taking advantage of GPU-based parallel codes. The free surfactant concentration was found to decrease rapidly as the total surfactant concentration increased, in agreement with the

present study of a fully atomistic model. The coarse-grained model of ref 85 predicts slightly higher CMCs than the values obtained in the present work but still underpredicts experimental data.

AUTHOR INFORMATION

Corresponding Author

*E-mail: azp@princeton.edu.

Notes

[§]Formerly M. Huhtala.

ACKNOWLEDGMENTS

This publication is based on work supported by the U.S. Department of Energy, Office of Basic Energy Sciences (Grant DE-SC-0002128). Additional support was provided by NSF-DMR Grant 0819860 (Princeton Center for Complex Materials). S.A.S. thanks David LeBard, Benjamin Levine, and Arben Jusufi for useful discussions. This research was supported by a Marie Curie Career Integration Grants within the 7th European Community Framework Programme, Academy of Finland, and CSC Finland (MS). Computations were performed at the TIGRESS facility jointly supported by the Princeton Institute for Computational Science and Engineering and the Princeton University Office of Information Technology.

REFERENCES

- (1) Peer, D.; Karp, J. M.; Hong, S.; Farokhzad, O. C.; Margalit, R.; Langer, R. *Nature. Nanotechnol.* **2007**, *2* (12), 751–760.
- (2) Torchilin, V. P. *Adv. Drug Delivery Rev.* **2006**, *58* (14), 1532–1555.
- (3) Yang, X. N.; Xu, Z. J.; Yang, Z. *Nano Lett.* **2010**, *10* (3), 985–991.
- (4) Blankschtein, D.; Lin, S. C. *J. Phys. Chem B* **2010**, *114* (47), 15616–15625.
- (5) Larson, R. G. *J. Chem. Phys.* **1988**, *89* (3), 1642–1650.
- (6) Mackie, A. D.; Onur, K.; Panagiotopoulos, A. Z. *J. Chem. Phys.* **1996**, *104* (10), 3718–3725.
- (7) Floriano, M. A.; Caponetti, E.; Panagiotopoulos, A. Z. *Langmuir* **1999**, *15* (9), 3143–3151.
- (8) Panagiotopoulos, A. Z.; Floriano, M. A.; Kumar, S. K. *Langmuir* **2002**, *18* (7), 2940–2948.
- (9) Al-Anber, S. A.; Avalos, J. B.; Floriano, M. A.; Mackie, A. D. *J. Chem. Phys.* **2003**, *118* (8), 3816–3826.
- (10) Cheong, D. W.; Panagiotopoulos, A. Z. *Langmuir* **2006**, *22* (9), 4076–4083.
- (11) Zheng, F. X.; Zhang, X. R.; Wang, W. C.; Dong, W. *Langmuir* **2006**, *22* (26), 11214–11223.
- (12) Davis, J. R.; Panagiotopoulos, A. Z. *J. Chem. Phys.* **2008**, *129* (19), 194706.
- (13) Davis, J. R.; Panagiotopoulos, A. Z. *J. Chem. Phys.* **2009**, *131* (11), 114901.
- (14) Smit, B.; Hilbers, P. A. J.; Esselink, K.; Rupert, L. A. M.; Vanos, N. M.; Schlijper, A. G. *J. Phys. Chem.* **1991**, *95* (16), 6361–6368.
- (15) Palmer, B. J.; Liu, J. *Langmuir* **1996**, *12* (3), 746–753.
- (16) Maillet, J. B.; Lachet, V.; Coveney, P. V. *Phys. Chem. Chem. Phys.* **1999**, *1* (23), 5277–5290.
- (17) Lyubartsev, A. P.; Rabinovich, A. L. *Soft Matter* **2011**, *7* (1), 25–39.
- (18) Mackerell, A. D. *J. Phys. Chem.* **1995**, *99* (7), 1846–1855.
- (19) Bandyopadhyay, S.; Tarek, M.; Lynch, M. L.; Klein, M. L. *Langmuir* **2000**, *16* (3), 942–946.
- (20) Tieleman, D. P.; van der Spoel, D.; Berendsen, H. J. C. *J. Phys. Chem. B* **2000**, *104* (27), 6380–6388.
- (21) Bruce, C. D.; Berkowitz, M. L.; Perera, L.; Forbes, M. D. E. *J. Phys. Chem. B* **2002**, *106* (15), 3788–3793.

- (22) Garde, S.; Yang, L.; Dordick, J. S.; Paulaitis, M. E. *Mol. Phys.* **2002**, *100* (14), 2299–2306.
- (23) Rakitin, A. R.; Pack, G. R. *J. Phys. Chem. B* **2004**, *108* (8), 2712–2716.
- (24) Sterpone, F.; Pierleoni, C.; Briganti, G.; Marchi, M. *Langmuir* **2004**, *20* (11), 4311–4314.
- (25) Boek, E. S.; Padding, J. T.; den Otter, W. K.; Briels, W. J. *J. Phys. Chem. B* **2005**, *109* (42), 19851–19858.
- (26) Piotrovskaya, E. M.; Vanin, A. A.; Smirnova, N. A. *Mol. Phys.* **2006**, *104* (22–24), 3645–3651.
- (27) Rose, D.; Rendell, J.; Lee, D.; Nag, K.; Booth, V. *Biophys. Chem.* **2008**, *138* (3), 67–77.
- (28) Marrink, S. J.; Tieleman, D. P.; Mark, A. E. *J. Phys. Chem. B* **2000**, *104* (51), 12165–12173.
- (29) Sammalkorpi, M.; Karttunen, M.; Haataja, M. *J. Phys. Chem. B* **2007**, *111* (40), 11722–11733.
- (30) Sammalkorpi, M.; Karttunen, M.; Haataja, M. *Chem. Phys. Lipids* **2007**, *149*, S87–S88.
- (31) Sammalkorpi, M.; Karttunen, M.; Haataja, M. *J. Am. Chem. Soc.* **2008**, *130* (52), 17977–17980.
- (32) Shelley, J. C.; Shelley, M. Y.; Reeder, R. C.; Bandyopadhyay, S.; Moore, P. B.; Klein, M. L. *J. Phys. Chem. B* **2001**, *105* (40), 9785–9792.
- (33) Marrink, S. J.; de Vries, A. H.; Mark, A. E. *J. Phys. Chem. B* **2004**, *108* (2), 750–760.
- (34) Izvekov, S.; Voth, G. A. *J. Phys. Chem. B* **2005**, *109* (7), 2469–2473.
- (35) Lyubartsev, A. P. *Eur. Biophys. J. Biophys. Lett.* **2005**, *35* (1), 53–61.
- (36) Marrink, S. J.; Risselada, H. J.; Yefimov, S.; Tieleman, D. P.; de Vries, A. H. *J. Phys. Chem. B* **2007**, *111* (27), 7812–7824.
- (37) Michel, D. J.; Cleaver, D. J. *J. Chem. Phys.* **2007**, *126* (3), 034506.
- (38) Shinoda, W.; Devane, R.; Klein, M. L. *Mol. Simul.* **2007**, *33* (1–2), 27–36.
- (39) Burov, S. V.; Obrezkov, N. P.; Vanin, A. A.; Piotrovskaya, E. M. *Colloid J.* **2008**, *70* (1), 1–5.
- (40) Orsi, M.; Haubertin, D. Y.; Sanderson, W. E.; Essex, J. W. *J. Phys. Chem. B* **2008**, *112* (3), 802–815.
- (41) Shinoda, W.; DeVane, R.; Klein, M. L. *Soft Matter* **2008**, *4* (12), 2454–2462.
- (42) Shinoda, W.; DeVane, R.; Klein, M. L. *Soft Matter* **2011**, *7* (13), 6178–6186.
- (43) Feig, M.; Brooks, C. L. *Curr. Opin. Struct. Biol.* **2004**, *14* (2), 217–224.
- (44) Lazaridis, T.; Mallik, B.; Chen, Y. *J. Phys. Chem. B* **2005**, *109* (31), 15098–15106.
- (45) Sanders, S. A.; Panagiotopoulos, A. Z. *J. Chem. Phys.* **2010**, *132* (11), 114902.
- (46) Jusufi, A.; Hynninen, A. P.; Panagiotopoulos, A. Z. *J. Phys. Chem. B* **2008**, *112* (44), 13783–13792.
- (47) Jusufi, A.; Sanders, S.; Klein, M. L.; Panagiotopoulos, A. Z. *J. Phys. Chem. B* **2011**, *115* (5), 990–1001.
- (48) Nielsen, S. O.; Lopez, C. F.; Srinivas, G.; Klein, M. L. *J. Phys.: Condens. Matter* **2004**, *16* (15), R481–R512.
- (49) Bock, H.; Gubbins, K. E. *Phys. Rev. Lett.* **2004**, *92* (13), 135701.
- (50) Van Gunsteren, W. F.; Berendsen, H. J. C. *Gromos-87 manual*; Biomos BV, Nijenborgh 4, 9747 AG Groningen, The Netherlands, 1987.
- (51) Berendsen, H. J. C.; Postma, J. P. M.; Van Gunsteren, W. F.; Hermans, J. In *Intermolecular Forces*; Pullman, B., Ed.; Reidel: Dordrecht: The Netherlands, 1981; pp 331–342.
- (52) Schweighofer, K. J.; Essmann, U.; Berkowitz, M. J. *J. Phys. Chem. B* **1997**, *101* (19), 3793–3799.
- (53) Martin, M. G.; Siepmann, J. I. *J. Phys. Chem. B* **1998**, *102* (14), 2569–2577.
- (54) Stubbs, J. M.; Siepmann, J. I.; Potoff, J. J. *J. Phys. Chem. B* **2004**, *108* (45), 17596–17605.
- (55) Kamath, G.; Potoff, J. J.; Cao, F. *J. Phys. Chem. B* **2004**, *108* (37), 14130–14136.
- (56) Cheng, T.; Chen, Q.; Li, F.; Sun, H. A. *J. Phys. Chem. B* **2010**, *114* (43), 13736–13744.
- (57) Abascal, J. L. F.; Vega, C. *J. Chem. Phys.* **2005**, *123* (23), 234505.
- (58) Vega, C.; Abascal, J. L. F.; Nezbeda, I. *J. Chem. Phys.* **2006**, *125* (3), 034503.
- (59) Vega, C.; de Miguel, E. *J. Chem. Phys.* **2007**, *126* (15), 154707.
- (60) Ghoufi, A.; Goujon, F.; Lachet, V.; Malfreyt, P. *J. Chem. Phys.* **2008**, *128* (15), 154716.
- (61) Mountain, R. D. *J. Phys. Chem. B* **2009**, *113* (2), 482–486.
- (62) Berendsen, H. J. C.; Grigera, J. R.; Straatsma, T. P. *J. Phys. Chem.* **1987**, *91* (24), 6269–6271.
- (63) Joung, I. S.; Cheatham, T. E. *J. Phys. Chem. B* **2008**, *112* (30), 9020–9041.
- (64) Sammalkorpi, M.; Sanders, S.; Panagiotopoulos, A. Z.; Karttunen, M.; Haataja, M. *J. Phys. Chem. B* **2011**, *115* (6), 1403–1410.
- (65) Fletcher, P. D. I.; Reinsborough, V. C. *Can. J. Chem.* **1981**, *59* (9), 1361–1367.
- (66) Rassing, J.; Sams, P. J.; Wynjones, E. *J. Chem. Soc., Faraday Trans. 2* **1973**, *69* (2), 180–185.
- (67) Rassing, J.; Sams, P. J.; Wynjones, E. *J. Chem. Soc., Faraday Trans. 2* **1973**, *70* (7), 1247–1258.
- (68) Aniansson, E. A. G.; Wall, S. N.; Almgren, M.; Hoffmann, H.; Kielmann, I.; Ulbricht, W.; Zana, R.; Lang, J.; Tondre, C. *J. Phys. Chem.* **1976**, *80* (9), 905–922.
- (69) Burov, S. V.; Vanin, A. A.; Brodskaya, E. N. *J. Phys. Chem. B* **2009**, *113* (31), 10715–10720.
- (70) Hess, B.; Kutzner, C.; van der Spoel, D.; Lindahl, E. *J. Chem. Theory Comput.* **2008**, *4* (3), 435–447.
- (71) Parrinello, M.; Rahman, A. *J. Appl. Phys.* **1981**, *52* (12), 7182–7190.
- (72) Nose, S.; Klein, M. L. *Mol. Phys.* **1983**, *50* (5), 1055–1076.
- (73) Hoover, W. G. *Phys. Rev. A* **1985**, *31* (3), 1695–1697.
- (74) Darden, T.; York, D.; Pedersen, L. *J. Chem. Phys.* **1993**, *98* (12), 10089–10092.
- (75) Essmann, U.; Perera, L.; Berkowitz, M. L.; Darden, T.; Lee, H.; Pedersen, L. G. *J. Chem. Phys.* **1995**, *103* (19), 8577–8593.
- (76) Kahlweit, M.; Teubner, M. *Adv. Colloid Interface Sci.* **1980**, *13* (1–), 1–64.
- (77) Johnson, I.; Olofsson, G.; Jonsson, B. *J. Chem. Soc., Faraday Trans. 1* **1987**, *83*, 3331–3344.
- (78) Polacek, R.; Kaatz, U. *J. Phys. Chem. B* **2007**, *111* (7), 1625–1631.
- (79) von Gottberg, F. K.; Smith, K. A.; Hatton, T. A. *J. Chem. Phys.* **1997**, *106* (23), 9850–9857.
- (80) Quina, F. H.; Nassar, P. M.; Bonilha, J. B. S.; Bales, B. L. *J. Phys. Chem.* **1995**, *99* (46), 17028–17031.
- (81) Soldi, V.; Keiper, J.; Romsted, L. S.; Cuccovia, I. M.; Chaimovich, H. *Langmuir* **2000**, *16* (1), 59–71.
- (82) Bales, B. L. *J. Phys. Chem. B* **2001**, *105* (29), 6798–6804.
- (83) Lebedeva, N. V.; Shahine, A.; Bales, B. L. *J. Phys. Chem. B* **2005**, *109* (42), 19806–19816.
- (84) Hsiao, C. C.; Wang, T. Y.; Tsao, H. K. *J. Chem. Phys.* **2005**, *122* (14), xxxx.
- (85) LeBard, D. N.; Levine, B. G.; Mertmann, P.; Barr, S. A.; Jusufi, A.; Sanders, S.; Klein, M. L.; Panagiotopoulos, A. Z. *Soft Matter* **2012**, DOI: 10.1039/C1SM06787G.
- (86) Adair, D. A. W.; Reinsbor, V.; Plavac, N.; Valteau, J. P. *Can. J. Chem.* **1974**, *52* (3), 429–433.
- (87) Ogino, K.; Kakihara, T.; Abe, M. *Colloid Polym. Sci.* **1987**, *265* (7), 604–612.
- (88) Hulsman, H. *Proc. K. Ned. Akad. Wet., Ser. B: Phys. Sci.* **1964**, *67* (367), xxxx.
- (89) Evans, H. C. *J. Chem. Soc.* **1956**, 579–586.
- (90) Israelachvili, J. N. *Intermolecular and Surface Forces*, 3rd ed.; Academic Press: Burlington, MA, 2011.

- (91) Patra, M.; Karttunen, M. *J. Comput. Chem.* **2004**, *25* (5), 678–689.
- (92) Jungwirth, P.; Tobias, D. J. *Chem. Rev.* **2006**, *106* (4), 1259–1281.
- (93) Jusufi, A.; LeBard, D. N.; Levine, B. G.; Klein, M. L. *J. Phys. Chem. B* **2012**, DOI: 10.1021/jp2102989.
- (94) Rafferty, J. L.; Sun, L.; Siepmann, J. I.; Schure, M. R. *Fluid Phase Equilib.* **2010**, *290* (1–2), 24–35.
- (95) Chen, B.; Siepmann, J. I.; Klein, M. L. *J. Am. Chem. Soc.* **2002**, *124* (41), 12232–12237.
- (96) Chen, B.; Siepmann, J. I. *J. Phys. Chem. B* **2006**, *110* (8), 3555–3563.